Simulating AC current transfer through near-electrode layers in very-high pressure arcs by means of COMSOL Multiphysics

N. A. Almeida and M. S. Benilov

Departamento de Física, CCCEE, Universidade da Madeira, 9000 Funchal, Portugal

Numerical simulation of AC current transfer through near-electrode layers in very-high pressure arcs in mercury and xenon is reported. The simulation is performed by means of a numerical model in which the whole of a near-electrode layer is simulated in the framework of a single set of equations without simplifying assumptions such as thermal equilibrium, ionization equilibrium, and quasi-neutrality. The system of equations includes equations of conservation of each species (the atoms, ions and electrons), transport equations for each species, equation of energy of the heavy species (the atoms and ions), equation of energy of the electrons, and the Poisson equation. The system of equations is solved numerically in 1D by means of a non-stationary solver of COMSOL Multiphysics.

1. Introduction

The plasma-electrode interaction in high-pressure arc discharges is dominated by non-LTE effects (e.g., [1] and references therein), which include a violation of thermal equilibrium, i.e., a divergence between the electron and heavy-particle temperatures; a violation of ionization equilibrium, i.e., a deviation of the charged-particle density from that predicted by the Saha equation; and a violation of quasi-neutrality, i.e., a divergence between the electron and ion number densities. A straightforward numerical calculation of near-electrode plasma layers with account of all these effects represents a difficult task. Therefore, in many works either some of these effects are discarded, or the near-electrode layer is *a priori* divided into a number of sub-layers, such as a layer of thermal non-equilibrium, an ionization layer, a near-electrode space-charge sheath etc, with each sub-layer being described by a separate set of equations and solutions in adjacent sub-layers being matched in some way or other at a boundary between the sub-layers (e.g., [1] and references therein).

Papers in which the whole of a near-electrode layer is simulated in the framework of a single set of equations with account of all the above-mentioned non-LTE effects have started to appear only recently [2, 3]. Such unified modelling approach does not rely on intuitive considerations, which are inevitable in models based on sub-layers and differ from one model to another, and is useful for developing commonly accepted physical understanding and/or simulation methods. This approach is independent of polarity and allows one to model both near-cathode and near-anode layers by means of the same code by merely changing sign of the current density; a feature important from the methodical point of view and essential for modelling near-electrode layers of AC arcs.

The unified modeling of near-cathode and near-anode layers was reported in [2] and [3], respectively. This work is concerned with modeling of near-electrode layers of AC arcs.

2. The model and numerics

The numerical model used in this work represents a non-stationary version of the model [2, 3]. The model takes into account the neutral atoms, ions, and electrons; the atoms and ions have the same temperature T_h which is in general different from the electron temperature T_e. The system of governing equations is as follows.

Equations of conservation of species read

$$\frac{\partial n_\alpha}{\partial t} + \nabla \cdot \mathbf{J}_\alpha = \omega_\alpha, \qquad \alpha = i, e, a, \qquad (1)$$

Here $\mathbf{J}_\alpha$ is the number density of transport flux of the species α ($\mathbf{J}_\alpha = n_\alpha \mathbf{v}_\alpha$, where n_α and $\mathbf{v}_\alpha$ are the number density and mean velocity of particles of the species α), ω_α is the net rate of production of particles of the species α in volume reactions, and indexes i, e, a refer to ions, electrons, and atoms, respectively. The dominating ionization mechanism in atomic plasmas is ionization in collisions with electrons and the dominating recombination mechanism is recombination with an electron acting as a third body, then

$$\omega_i = \omega_e = -\omega_a = k_i n_a n_e - k_r n_i n_e^2, \qquad (2)$$

where k_i and k_r are the ionization and recombination rate constants.

The transport equations for species are written in the form of hydrodynamic Stefan-Maxwell equations (e.g., [4, 5] and references therein), which are applicable at any ionization degree of the plasma.

$$-\nabla p_\alpha + n_\alpha e Z_\alpha \mathbf{E} + \frac{\rho_\alpha}{\rho}\left[\nabla p - e\left(n_i - n_e\right)\mathbf{E}\right] - \sum_\beta \frac{n_\alpha n_\beta k T_{\alpha\beta} C_{\alpha\beta}}{n D_{\alpha\beta}}\left(\mathbf{v}_\alpha - \mathbf{v}_\beta\right) - \mathbf{R}_\alpha^T = 0, \quad (3)$$

where

$$m_{\alpha\beta} = \frac{m_\alpha m_\beta}{m_\alpha + m_\beta}, \quad T_{\alpha\beta} = \frac{m_\alpha T_\beta + m_\beta T_\alpha}{m_\alpha + m_\beta}. \quad (4)$$

Here $\alpha, \beta = i, e, a$; m_α, T_α, $\rho_\alpha = n_\alpha m_\alpha$, and $p_\alpha = n_\alpha k T_\alpha$ are the particle mass, temperature, mass density, and partial pressure of the species α; $n = \sum_\beta n_\beta$, $\rho = \sum_\beta \rho_\beta$, and $p = \sum_\beta p_\beta$ are the total number and mass densities and pressure of the plasma; $D_{\alpha\beta}$ are binary diffusion coefficients evaluated in the first approximation in expansion in the Sonine polynomials in the method of Chapman–Enskog and $C_{\alpha\beta}$ are coefficients of the order unity introducing corrections arising in higher approximations (note that $D_{\beta\alpha} = D_{\alpha\beta}$, $C_{\beta\alpha} = C_{\alpha\beta}$); $m_{\alpha\beta}$ and $T_{\alpha\beta}$ are the reduced mass and temperature; terms $\mathbf{R}_\alpha^T$ account for thermal diffusion; $\mathbf{E}$ is the electric field.

The thermal diffusion forces $\mathbf{R}_\alpha^T$ are given by formulas

$$\mathbf{R}_\alpha^T = C_\alpha^{(h)} n_\alpha k \nabla T_h + C_\alpha^{(e)} n_\alpha k \nabla T_e, \; \mathbf{R}_e^T = C_e^{(e)} n_e k \nabla T_e \quad (5)$$

for heavy-particle species ($\alpha = i, a$) and for electrons, respectively. (Note that the transport equation for electrons does not contain a term with ∇T_h since the corresponding force is negligibly small due to the smallness of the electron-to-ion mass ratio [4]). The thermal diffusion coefficients $C_\alpha^{(h)}$ and $C_\alpha^{(e)}$ satisfy equalities

$$n_a C_a^{(h)} + n_i C_i^{(h)} = 0, \quad \sum_\alpha n_\alpha C_\alpha^{(e)} = 0. \quad (6)$$

Equations (3) are dependent (summation of these equations over α gives a trivial result), therefore any one of them may be dropped. We will drop the equation for atoms.

The electron and heavy-particle energy equations can be written as [6]

$$\frac{\partial}{\partial t}\left(n_e \frac{3}{2} k T_e\right) + \nabla \cdot \left(\frac{5}{2} k T_e \mathbf{J}_e + \mathbf{h}_e\right) = -e\mathbf{J}_e \cdot \mathbf{E} - \frac{3 n_e k^2 T_e}{m_i n}\left(T_e - T_h\right)\left(\frac{n_a}{D_{ea}} + \frac{n_i}{D_{ei}}\right) - w_e^{(e)}, \quad (7)$$

$$\frac{\partial}{\partial t}\left(\left(n_i + n_a\right)\frac{3}{2} k T_h\right) + \nabla \cdot \left(\frac{5}{2} k T_h \mathbf{J}_a + \frac{5}{2} k T_h \mathbf{J}_i + \mathbf{h}_{hp}\right) = e\mathbf{J}_i \cdot \mathbf{E} + \frac{3 n_e k^2 T_e}{m_i n}\left(T_e - T_h\right)\left(\frac{n_a}{D_{ea}} + \frac{n_i}{D_{ei}}\right), \quad (8)$$

where $\mathbf{h}_e$ and $\mathbf{h}_{hp}$ are the densities of heat fluxes transported by the electrons and heavy particles, respectively. The terms with the factor 5/2 on the left-hand side of each of these equations account for the enthalpy transport by the diffusion fluxes. The first term on the right-hand side accounts for Joule heating of the electron or, respectively, ion species. The second term accounts for the energy exchange between the electrons and the heavy particles due to elastic collisions. The third term on the right-hand side of equation (7) accounts for losses of electron energy due to inelastic collisions and may be written as [6]

$$w_e^{(e)} = A_i \omega_e + w_{rad}, \quad (9)$$

where A_i is the energy of ionization of an atom and w_{rad} designates losses of electron energy through radiation or, in other words, the net emission coefficient (e.g., [7, 8]) integrated over the solid angle.

Densities of electron and heavy-particle heat fluxes represent a combination of heat fluxes caused by heat conduction and by the effect inverse to the thermal diffusion, and are written as [4]

$$\mathbf{h}_e = -\kappa_e \nabla T_e + k T_e n_e \left[A_i^{(e)}\left(\mathbf{v}_e - \mathbf{v}_i\right) + A_a^{(e)}\left(\mathbf{v}_e - \mathbf{v}_a\right)\right], \quad (10)$$

$$\mathbf{h}_{hp} = -\kappa_{hp} \nabla T_h + k T_h \left[n_i A_i^{(h)}\left(\mathbf{v}_i - \mathbf{v}_a\right) + n_a A_a^{(h)}\left(\mathbf{v}_a - \mathbf{v}_i\right)\right], \quad (11)$$

where κ_e and κ_{hp} are thermal conductivities of the electron and heavy-particle gases and $A_i^{(e)}$, $A_a^{(e)}$, $A_i^{(h)}$, and $A_a^{(h)}$ are kinetic coefficients.

The set of equations includes also the Poisson equation, which is written as

$$\varepsilon_0 \nabla \cdot \mathbf{E} = e\left(n_i - n_e\right). \quad (12)$$

The modelling results reported in this work refer to the case of parallel-plane current transfer to a planar electrode through a planar near-electrode region. The pressure is considered constant and is considered as an input parameter.

The boundary conditions at the electrode surface are the same as in [2] and take into account

the emission of electrons by the surface. Since the current density is constant in the planar geometry, all parameters of the plasma (except the electrostatic potential) are constant at large distances from the electrode, where the plasma is in the state of local thermodynamic equilibrium, or LTE and its energy balance is dominated by radiation. One can say that the plasma far from the electrode is not disturbed by the electrode. The upper boundary of the calculation domain is positioned far enough from the electrode surface in the undisturbed plasma and the conditions at this boundary are zero derivatives.

The above-stated problem is solved by means of a non-stationary solver of COMSOL Multiphysics. The plasma-producing gas is Xe or Hg. The transport and kinetic coefficients are the same as those in [2, 3]. Note that test calculations performed by means of the same code with a constant (time independent) current density by means of a stationary solver gave results exactly coinciding with those obtained for near-cathode and near-anode layers of DC arcs by a stationary Fortran code used in [2, 3].

3. Results and discussion

As an example, let us consider results of calculations for a very-high pressure (100 bar) Xe arc with the current density j being a square-wave function of time t with an amplitude of $10^5\,\mathrm{A\,m^{-2}}$ and frequency, f, of $10^4\,\mathrm{Hz}$ (the rise/fall time of j was chosen as $f/10$). In the simulations it was assumed that the electrodes were made of pure tungsten and that the temperature of the electrode surface was $T_w = 3000\,\mathrm{K}$. The results of the simulations are the following. In figure 1 the potential difference between the electrode and the upper boundary of the calculation domain is represented as a function of time together with the current density. In this and in the following figures positive values of j represent calculations for the cathodic phase and negative values represent the anodic phase. Is it worth mentioning that because of the high frequency of the square-wave current density in each phase the potential difference does not have enough time to stabilize to the stationary value.

In figures 2 and 3 is shown respectively the density and the temperature of the electrons at the electrode surface.

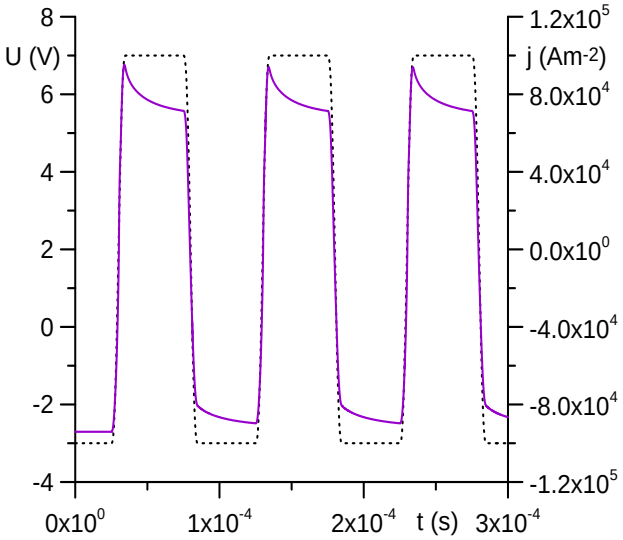

Figure 1. Potential difference between the electrode and the upper boundary of the calculation domain as a function of time. Solid lines: Potential difference between the electrode and the upper boundary of the calculation domain. Dashed lines: The applied current density j.

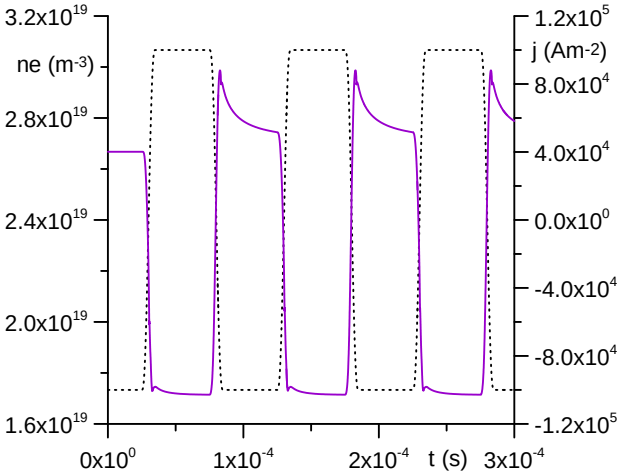

Figure 2. Density of the electrons at the electrode surface as a function of time. Solid lines: Density of electrons at the electrode surface. Dashed lines: The applied current density j.

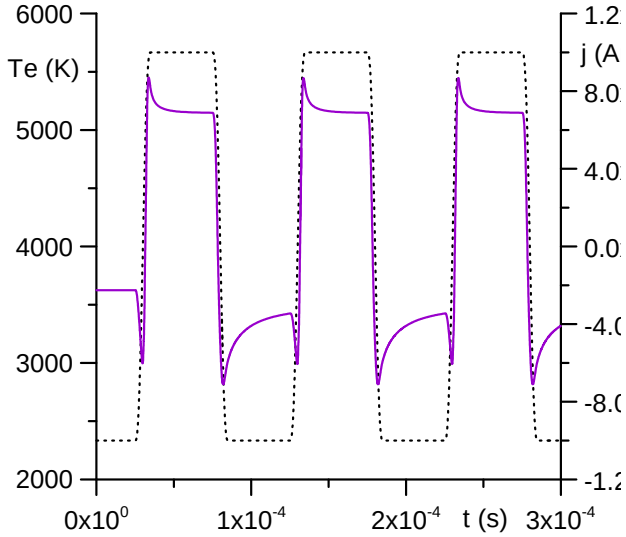

Figure 3. Temperature of the electrons at the electrode surface as a function of time. Solid lines: Temperature of electrons at the electrode surface. Dashed lines: The applied current density j.

Acknowledgments This work was supported by FCT through the projects PTDC/FIS-PLA/2708/2012 and PEst-OE/MAT/UI0219/2011.

4. References

[1] M. S. Benilov, J. Phys. D: Appl. Phys. **41** (2008) 144001.

[2] N. A. Almeida, M. S. Benilov, and G. V. Naidis, J. Phys. D: Appl. Phys. **41** (2008) 245201.

[3] N. A. Almeida, M. S. Benilov, U. Hechtfischer, and G. V. Naidis, J. Phys. D: Appl. Phys. **42** (2009) 045210.

[4] V. M. Zhdanov, *Transport Phenomena in Multi-component Plasma* (Taylor and Francis, London and New York, 2002).

[5] V. Rat *et al.*, J. Phys. D: Appl. Phys. **41** (2008) 183001.

[6] M. Mitchner and C. H. Kruger, *Partially Ionized Gases* (Wiley, New York, 1973).

[7] J. J. Lowke, J. Appl. Phys. **41** (1970) 2588 .

[8] A. Gleizes, J. J. Gonzalez, and P. Freton, J. Phys. D: Appl. Phys. **38** (2005) R153.